

# Sliding Mode Control Improvement by using Model Predictive, Fuzzy Logic, and Integral Augmented Techniques for a Quadrotor Helicopter Model

Amir Hossein Zaeri<sup>1</sup>, Aida Esmaeilian-Marnani<sup>2\*</sup>, Samsul Bahari Mohd Noor<sup>3</sup>  
1- Department of Electrical Engineering, Shahinshahr Branch, Islamic Azad University, Shahinshahr, Iran.

Email: amzaeri@gmail.com (Corresponding author)

2- Department of Electrical and Computer Engineering, Mobarakeh Branch, Islamic Azad University, Mobarakeh, Isfahan, Iran.  
Email: ai\_esmailian@yahoo.com

3- Department of Electrical and Electronic Engineering, Faculty of Engineering, University Putra Malaysia, Serdang, Malaysia.  
Email: samsul@eng.upm.edu.my

Received: February 2019

Revised: June 2019

Accepted: August 2019

## ABSTRACT:

In this paper, a new control method is adopted based on merging multi-input Integral Sliding Mode Control with Boundary Layer (ISMC-BL), Model Predictive Control (MPC), and Fuzzy Logic Control (FLC). The aim of this merging is to take advantage of MPC ability to deal with constraints and to gain optimal solution. Moreover, FLC is considered in designing the sliding surface based on fuzzy rules and tracking error. This method is simulated on a nonlinear quadrotor helicopter model. The results have revealed that the proposed control approach, which is a multi-input Model Predictive Fuzzy Integral Sliding Mode Control with Boundary Layer (MPFISMC-BL), is a robust, stable, optimal, and intelligent control scheme. This finding could contribute to improve the control of similar systems.

**KEYWORDS:** Quadrotor Helicopter, Model Predictive Control, Sliding Mode Control, Fuzzy Logic Control.

## 1. INTRODUCTION

Autonomous unmanned aerial vehicles (UAV) have attracted many researchers due to their vast applications such as where safety is important or there is a confrontation with natural risks. In addition, it can be used in environmental protection and exploration, traffic surveillance, structure inspection, mapping, agriculture, film production, and aerial cinematography. These vehicles have low cost and reduced radar signatures, compared to manned vehicles. A quadrotor is a four-rotor six-degree-of-freedom (6-DOF) UAV helicopter which is under the focus of many researchers due to their capability of landing and taking off vertically in hovering.

Multi-input sliding mode control (SMC) is a robust controller that can be used to control linear and nonlinear plants to achieve desired performance in the presence of uncertainty and disturbance [1-4]. Moreover, its stability is proven by Lyapunov's theorem.

In practical applications, SMC suffers from problems such as chattering, which increases the control effort that may lead to instability of the system. In addition, the SMC parameters are off-line and cannot be optimized. Improvement of SMC has been investigated by many researchers. One important

suggested method, which could update some SMC parameters online, is model predictive sliding mode control (MPSMC) achieved by merging SMC and model predictive control (MPC) [5]. This approach is also confronted with some problems especially due to complicated calculations and conservative strategy of nonlinear MPC for a nonlinear system at each sampling time.

This paper relates improvement of sliding mode controller performance by introducing a new strategy to merge SMC with linear MPC and fuzzy logic control (FLC). Boundary layer and integral augmented are also exploited.

The model tested under different controllers, is a nonlinear quadrotor helicopter model as a four-rotor 6-DOF helicopter, which is a kind of autonomous unmanned aerial vehicle (UAV) system. The results of improved SMC are compared with those of an integral predictive nonlinear  $H_\infty$  control for this system.

## 2. REVIEW OF RESEARCH ON QUADROTOR HELICOPTER

Quadrotor, as a real unmanned vehicle model (UAV), has been an attractive model for study by many researchers in recent years. Different methods are employed to control quadrotor helicopters. Sliding

mode control is suggested by some researches [1-4]. However, chattering is a serious problem for such methods. Intelligent control algorithms, such as fuzzy logic, neural network, and genetic algorithm, are also employed in some control approaches [6-8].  $H_\infty$  is an optimal control algorithm utilized for quadrotor control [9]. Each algorithm deals with problems clarified in the introduction section.

In this paper, some algorithms are combined to overcome the algorithm constraints. Quadrotor model is considered for comparing the results of the proposed control method with those of integral predictive nonlinear  $H_\infty$  control method.

### 3. METHODOLOGY

#### 3.1. Quadrotor Helicopter

It is important to consider the dynamics of 6-DOF quadrotor helicopter for gravity effects and aerodynamic forces. Configuration of considered quadrotor helicopter is illustrated in Fig. 1.

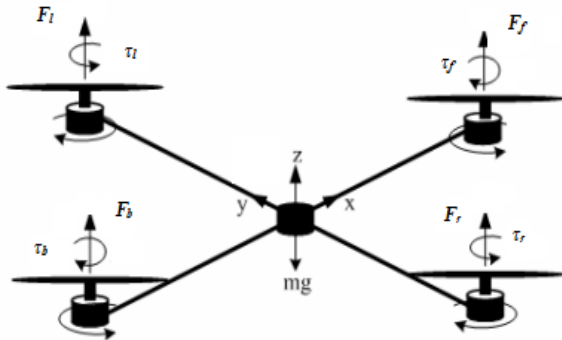


Fig. 1. Configuration of quadrotor helicopter [9].

Quadrotor movement is due to the adjusting of rotor velocity that changes the lift force. Longitudinal movements are due to the front and back rotor velocities that changes the forces  $F_f$  and  $F_b$ , as shown in Fig. 1. In addition, lateral movement is due to the speed of the right and left propellers, which changes the forces  $F_r$  and  $F_l$ . Yaw movement results from the difference in the counter-torque between each pair of propellers, ( $F_f$ ,  $F_b$ ) and ( $F_r$ ,  $F_l$ ). In other words, it is due to accelerating the two clockwise turning rotors while decelerating the counter clockwise turning rotors, and vice versa. The helicopter movement results from the sum of the four forces [9].

Therefore, the total force  $F_f$ , rolling torque  $\tau_\phi$ , pitching torque  $\tau_\theta$ , and yawing torque  $\tau_\psi$ , can be respectively written as

$$F = F_f + F_r + F_b + F_l \quad (1)$$

$$\tau_\phi = l(F_l - F_r) \quad (2)$$

$$\tau_\theta = l(F_f - F_b) \quad (3)$$

$$\tau_\psi = \tau_r + \tau_l - \tau_f - \tau_b \quad (4)$$

Where, torques and forces are shown in Fig. 1.

$-\pi/2 < \theta < \pi/2$ ,  $-\pi < \varphi < \pi$ , and  $-\pi/2 < \psi < \pi/2$  are rotational angels, pitch, yaw, and roll, respectively.  $l$  is the center of mass length along helicopter body from pitch axis.

#### 3.2. MPFISM-C-BL Design for Quadrotor Helicopter

The mathematical rotational movement and the translational movement obtained from the Lagrange-Euler formalism as well as external disturbance for a quadrotor helicopter are considered as following [9]:

$$\begin{cases} \ddot{x} = \frac{1}{m} (\cos \psi \sin \theta \cos \varphi + \sin \psi \sin \varphi) U + \frac{A_x}{m} \\ \ddot{y} = \frac{1}{m} (\sin \psi \sin \theta \cos \varphi - \cos \psi \sin \varphi) U + \frac{A_y}{m} \\ \ddot{z} = -g + \frac{1}{m} (\cos \theta \cos \varphi) U + \frac{A_z}{m} \end{cases} \quad (5)$$

$$\begin{bmatrix} \dot{\phi} \\ \dot{\theta} \\ \dot{\psi} \end{bmatrix} = \begin{bmatrix} 1 & \sin \varphi \tan \theta & \cos \varphi \tan \theta \\ 0 & \cos \varphi & -\sin \varphi \\ 0 & \sin \varphi \sec \theta & \cos \varphi \sec \theta \end{bmatrix} \begin{bmatrix} p \\ q \\ r \end{bmatrix} \quad (6)$$

Where,  $x$ ,  $y$ , and  $z$  represent the helicopter mass center position. vector  $\mathbf{A}=[A_x \ A_y \ A_z \ A_p \ A_q \ A_r]$  is the external disturbance vector. Vectors  $[\phi \ \theta \ \psi]'$  and  $[p \ q \ r]'$  are the angular velocities. Moreover,  $-\pi/2 < \theta < \pi/2$ ,  $-\pi < \varphi < \pi$ , and  $-\pi/2 < \psi < \pi/2$  are rotational angels, pitch, yaw, and roll, respectively.  $m$  is the helicopter mass.  $g$  is the gravitational acceleration.  $U$  is the main control input. In this case, by considering a small variation of roll angle, equation (5) can be approximated as [10].

$$\begin{cases} \ddot{x} = \frac{1}{m} (\sin \theta \cos \varphi) U + \frac{A_x}{m} \\ \ddot{y} = \frac{-1}{m} (\sin \varphi) U + \frac{A_y}{m} \\ \ddot{z} = -g + \frac{1}{m} (\cos \theta \cos \varphi) U + \frac{A_z}{m} \end{cases} \quad (7)$$

$$\begin{cases} \ddot{\phi} = \frac{1}{J_x} \tau_\phi + \frac{A_p}{J_x} \\ \ddot{\theta} = \frac{1}{J_y} \tau_\theta + \frac{A_q}{J_y} \\ \ddot{\psi} = \frac{1}{J_z} \tau_\psi + \frac{A_r}{J_z} \end{cases} \quad (8)$$

In equations (2) to (4), the relations between torques and forces, which are applied to quadrotor motors, are defined.

In order to simplify the equations and consider a linear system without coupling, it is supposed that [9]

$$\begin{cases} u_x = \frac{1}{m}(\cos\psi \sin\theta \cos\varphi + \sin\psi \sin\varphi)U \\ u_y = \frac{1}{m}(\sin\psi \sin\theta \cos\varphi - \cos\psi \sin\varphi)U \\ u_z = -g + \frac{1}{m}\cos\theta \cos\varphi U \end{cases} \quad (9)$$

Equation (9) show that  $u_x$  and  $u_y$  are used as the direction of  $U$  where respectively causes the movements through the  $x$  and  $y$  axes. Besides, equation (7) can be changed to

$$\begin{cases} \ddot{x} = u_x + d_x \\ \ddot{y} = u_y + d_y \\ \ddot{z} = u_z + d_z \end{cases} \quad (10)$$

From equation (9),  $U$  and the desired pitch and roll angles can be written as follows:

$$\frac{U}{m} = \frac{u_z + g}{\cos\theta \cos\varphi} \quad (11)$$

$$\theta_d = \sin^{-1}\left(\frac{u_x - \sin\psi \sin\varphi_d}{\cos\psi \cos\varphi_d}\right) \quad (12)$$

$$\varphi_d = \sin^{-1}(u_x \sin\psi - u_y \cos\psi) \quad (13)$$

Therefore, the equations of the desired pitch and roll angles consider the coupling between the different parts of the system and nonlinearity for the quadrotor helicopter model.

In order to design ISMC-BL for quadrotor helicopter, equations (8) and (10) are employed. Moreover, A nonlinear multi-input system is considered of the form

$$\begin{aligned} x_i^{(n_i)} &= f_i(\mathbf{x}) + \sum_{j=1}^m b_{ij}(\mathbf{x})u_j \\ i &= 1, \dots, m \quad j = 1, \dots, m \end{aligned} \quad (14)$$

Therefore, matrix  $\mathbf{f}$  and  $\mathbf{B}$  can be calculated as

$$\mathbf{f} = \begin{bmatrix} f_1 \\ f_2 \\ f_3 \\ f_4 \\ f_5 \\ f_6 \end{bmatrix} = \mathbf{0}, \quad \mathbf{B} = I_{6 \times 6} \quad (15)$$

Where,

$$\mathbf{x}^T = [x, y, z, \psi, \theta, \varphi] \quad (16)$$

The basic ISMC-BL design procedure is performed in two steps. First, the choice of sliding surface,  $s$ , according to the tracking error, is followed. In the second step, design of the control law, which can satisfy the stability sliding condition ( $s\dot{s} < 0$ ), is considered. Sliding surface can be calculated for each single input as,

$$s_x = \dot{\tilde{x}} + \lambda_x \tilde{x} + k_{I_x} \int_0^t \tilde{x}(\tau) d\tau \quad (17)$$

$$s_z = \dot{\tilde{z}} + \lambda_z \tilde{z} + k_{I_z} \int_0^t \tilde{z}(\tau) d\tau \quad (18)$$

$$s_\varphi = \dot{\tilde{\varphi}} + \lambda_\varphi \tilde{\varphi} + k_{I_\varphi} \int_0^t \tilde{\varphi}(\tau) d\tau \quad (19)$$

$$s_\theta = \dot{\tilde{\theta}} + \lambda_\theta \tilde{\theta} + k_{I_\theta} \int_0^t \tilde{\theta}(\tau) d\tau \quad (20)$$

$$s_\psi = \dot{\tilde{\psi}} + \lambda_\psi \tilde{\psi} + k_{I_\psi} \int_0^t \tilde{\psi}(\tau) d\tau \quad (21)$$

Where,

$$\begin{bmatrix} \tilde{x} \\ \tilde{y} \\ \tilde{z} \\ \tilde{\varphi} \\ \tilde{\theta} \\ \tilde{\psi} \end{bmatrix} = \begin{bmatrix} x - x_d \\ y - y_d \\ z - z_d \\ \varphi - \varphi_d \\ \theta - \theta_d \\ \psi - \psi_d \end{bmatrix} \quad (22)$$

The control law for ISMC-BL is obtained as

$$u_x = \ddot{x}_d - \lambda_x \dot{\tilde{x}} - k_{I_x} \tilde{x} - k_x \text{sat}\left(\frac{s_x}{\beta_x}\right) \quad (23)$$

$$u_y = \ddot{y}_d - \lambda_y \dot{\tilde{y}} - k_{I_y} \tilde{y} - k_y \text{sat}\left(\frac{s_y}{\beta_y}\right) \quad (24)$$

$$u_z = \ddot{z}_d - \lambda_z \dot{\tilde{z}} - k_{I_z} \tilde{z} - k_z \text{sat}\left(\frac{s_z}{\beta_z}\right) \quad (25)$$

$$u_\varphi = \ddot{\varphi}_d - \lambda_\varphi \dot{\tilde{\varphi}} - k_{I_\varphi} \tilde{\varphi} - k_\varphi \text{sat}\left(\frac{s_\varphi}{\beta_\varphi}\right) \quad (26)$$

$$u_\theta = \ddot{\theta}_d - \lambda_\theta \dot{\tilde{\theta}} - k_{I_\theta} \tilde{\theta} - k_\theta \text{sat}\left(\frac{s_\theta}{\beta_\theta}\right) \quad (27)$$

$$u_\psi = \ddot{\psi}_d - \lambda_\psi \dot{\tilde{\psi}} - k_{I_\psi} \tilde{\psi} - k_\psi \text{sat}\left(\frac{s_\psi}{\beta_\psi}\right) \quad (28)$$

In order to use MPFISMC-BL, switching gains  $\mathbf{k} = [k_x \ k_y \ k_z \ k_\varphi \ k_\theta \ k_\psi]$  are designed using

MPC. The cost functions, which include sliding surface errors and control efforts, are obtained as follows

$$J_x = \sum_{j=0}^{N_p} \mu_{s_x}(j)[s_x^2(t+j)] + \sum_{j=0}^{N_c} \mu_{k_x}(j)[k_x(t+j) - k_x(t+j-1)]^2 \quad (29)$$

$$J_y = \sum_{j=0}^{N_p} \mu_{s_y}(j)[s_y^2(t+j)] + \sum_{j=0}^{N_c} \mu_{k_y}(j)[k_y(t+j) - k_y(t+j-1)]^2 \quad (30)$$

$$J_z = \sum_{j=0}^{N_p} \mu_{s_z}(j)[s_z^2(t+j)] + \sum_{j=0}^{N_c} \mu_{k_z}(j)[k_z(t+j) - k_z(t+j-1)]^2 \quad (31)$$

$$J_\phi = \sum_{j=0}^{N_p} \mu_{s_\phi}(j)[s_\phi^2(t+j)] + \sum_{j=0}^{N_c} \mu_{k_\phi}(j)[k_\phi(t+j) - k_\phi(t+j-1)]^2 \quad (32)$$

$$J_\theta = \sum_{j=0}^{N_p} \mu_{s_\theta}(j)[s_\theta^2(t+j)] + \sum_{j=0}^{N_c} \mu_{k_\theta}(j)[k_\theta(t+j) - k_\theta(t+j-1)]^2 \quad (33)$$

$$J_\psi = \sum_{j=0}^{N_p} \mu_{s_\psi}(j)[s_\psi^2(t+j)] + \sum_{j=0}^{N_c} \mu_{k_\psi}(j)[k_\psi(t+j) - k_\psi(t+j-1)]^2 \quad (34)$$

To satisfy the stability condition, it is necessary to

consider constraints on designing switching gains by MPC. In this case,  $k_{i,min}$  is calculated by considering maximum value of disturbance as follows

$$\gamma_i + \eta_i \leq k_i \leq k_{i,max} \quad (35)$$

In this approach, sliding surfaces for pitch and yaw angles,  $\lambda_\theta$  and  $\lambda_\psi$ , are obtained using FLC. By considering the effect of  $\lambda$  on tracking error, fuzzy lows are written in Table 1. In order to reduce the method complication and calculation, one fuzzy input and output are selected for each rotational axes.

**Table 1.** Fuzzy rules for rotational movement of quadrotor.

If $e_\phi$ is P then $\lambda_\phi$ is L	If $e_\phi$ is N then $\lambda_\phi$ is L
If $e_\phi$ is Z then $\lambda_\phi$ is S	If $e_\theta$ is P then $\lambda_\theta$ is L
If $e_\theta$ is N then $\lambda_\theta$ is L	If $e_\theta$ is Z then $\lambda_\theta$ is S

Fig. 2 shows the block diagram of quadrotor helicopter using MPFISM-C-BL. Control method details for translational and rotational movement are illustrated in this figure.

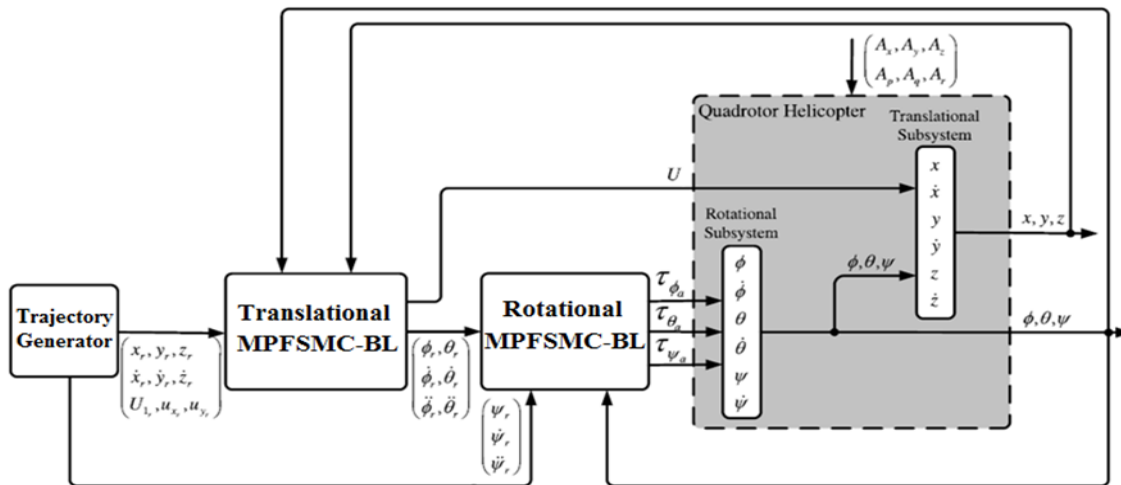


**Fig. 2.** Structure of quadrotor helicopter using MPFISM-C-BL control.

#### 4. RESULTS AND DISCUSSION

A quadrotor helicopter is employed for testing the proposed controller, MPFISM-C-BL. The mathematical model of the plant is based on equations (8) and (10) [9].

In order to compare the proposed controller with another nonlinear, predictive and optimal controller, which is an integral predictive/nonlinear  $H_\infty$  controller, following simulation is performed [9]. The initial

conditions of the helicopter are  $[x(0) \ y(0) \ z(0) \ \phi(0) \ \theta(0) \ \psi(0)] = [0 \ \text{m} \ 0.5 \ \text{m} \ 0.5 \ \text{m} \ 0 \ \text{rad} \ 0 \ \text{rad} \ 0.5 \ \text{rad}]$ . The values of the model parameters used for simulations are  $m = 0.74 \ \text{kg}$ ,  $g = 9.81 \ \text{m/s}^2$ .

In considering the thrust value  $U \approx 7.23 \ \text{N}$  for hovering flight of quadrotor helicopter under ideal conditions, the persistent light gusts of wind, which are supposed as external disturbances on the aerodynamic forces and moments, are  $A_x = 1 \ \text{N}$  at  $t = 5 \ \text{s}$ ,  $A_p = 1 \ \text{Nm}$

at  $t = 10\text{ s}$ ,  $A_y = 1\text{ N}$  at  $t = 15\text{ s}$ ,  $A_q = 1\text{ Nm}$  at  $t = 20\text{ s}$ ,  $A_z = 1\text{ N}$  at  $t = 25\text{ s}$ , and  $A_r = 1\text{ Nm}$  at  $t = 30\text{ s}$  [9]. Fig. 3

depicts these external transactional and angular disturbances.

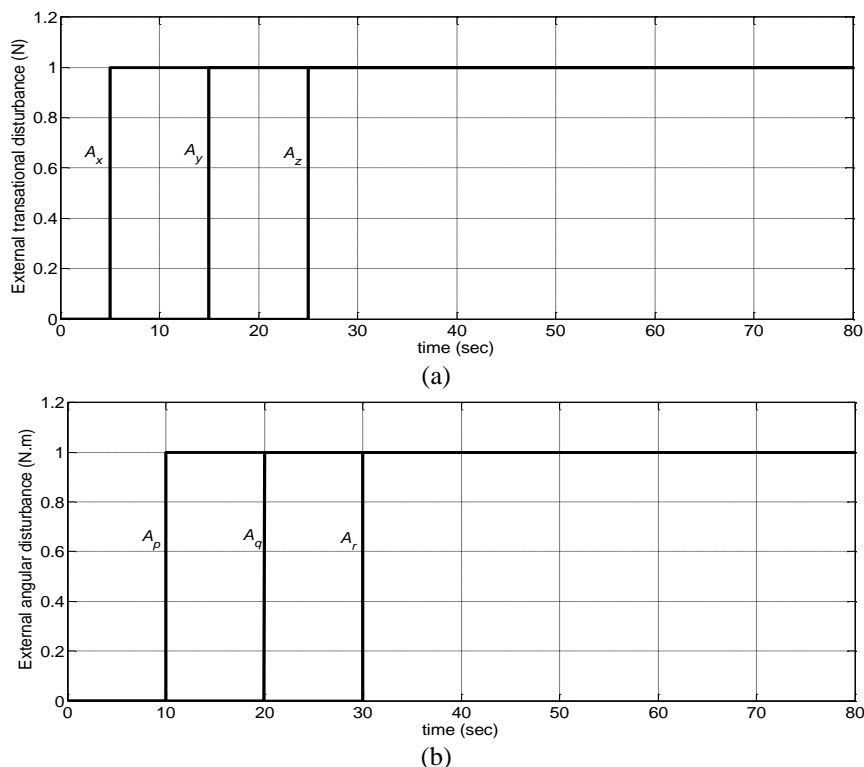


Fig. 3. (a) External transactional and (b) external angular disturbances.

In simulation, a reference trajectory, which is considered with several kinds of stretches, starts from  $x_r(0) = 0.5\text{ m}$ ,  $y_r(0) = 0\text{ m}$ ,  $z_r(0) = 1\text{ m}$ , and  $\psi_r(0) = 0\text{ rad}$ . In this case, because of the appearing steady state error, MPFISM is applied to the system by considering  $k_{Iz} = 2$ ,  $k_{I\psi} = 0.14$ , while other integral gains equal to 1. The new parameters of MPC for all degrees, except for  $\varphi$  and  $\theta$ , are presented in Table 2.

Table 2. MPC parameters of MPFISM-BL for quadrotor helicopter.

Sample time	$T_s = 0.1\text{ sec}$
Predictive horizon	$N_p = 10$
Control horizon	$N_c = 2$
Down switching gain limitation	$k_{sw,min} = 1$
Up switching gain limitation	$k_{sw,max} = 15$

In order to consider nonlinearity of system for desired inputs of  $\varphi$  and  $\theta$ , the up switching gain limitations are supposed to be smaller than other degrees and equal to 10. The boundary layers of all degrees are equal to 1. The fuzzy membership functions for designing sliding surface slopes of  $\varphi$  and  $\theta$  are shown in Fig. 4. The  $\lambda_z$  is equal to 1.6 and other sliding surface slopes are equal to 1. The simulation results are depicted in Figs. 5, 6, and 7. These figures

show that the control strategy properly follows the path, despite the system suffering abrupt changes in the reference and disturbances.

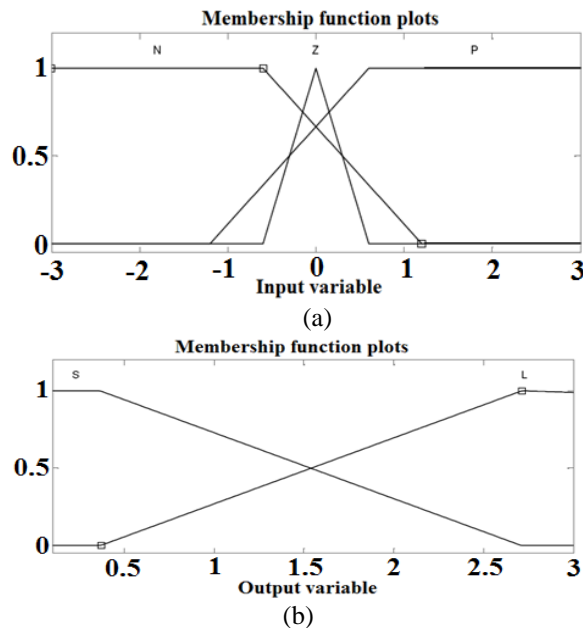


Fig. 4. Input and output fuzzy membership functions, a) input and b) output variables.

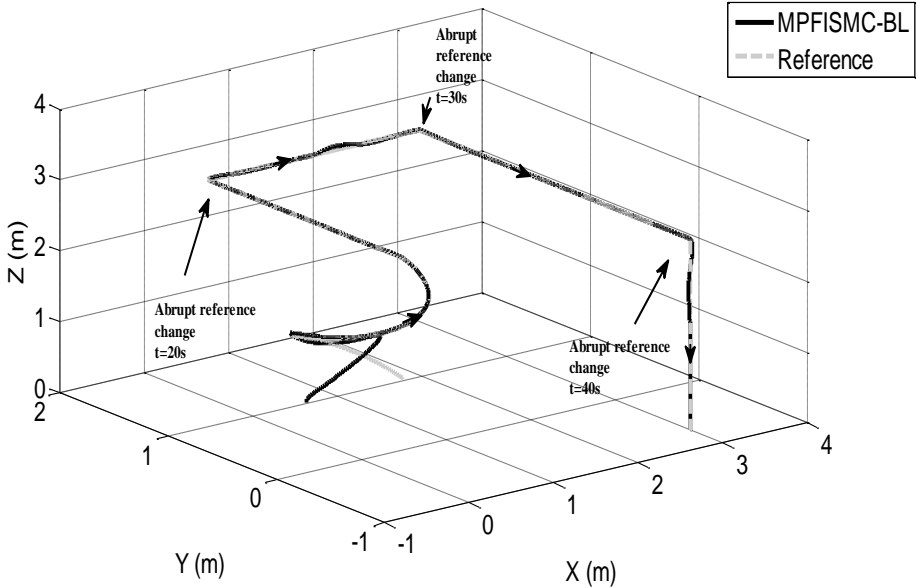


Fig. 5. Path following for quadrotor helicopter.

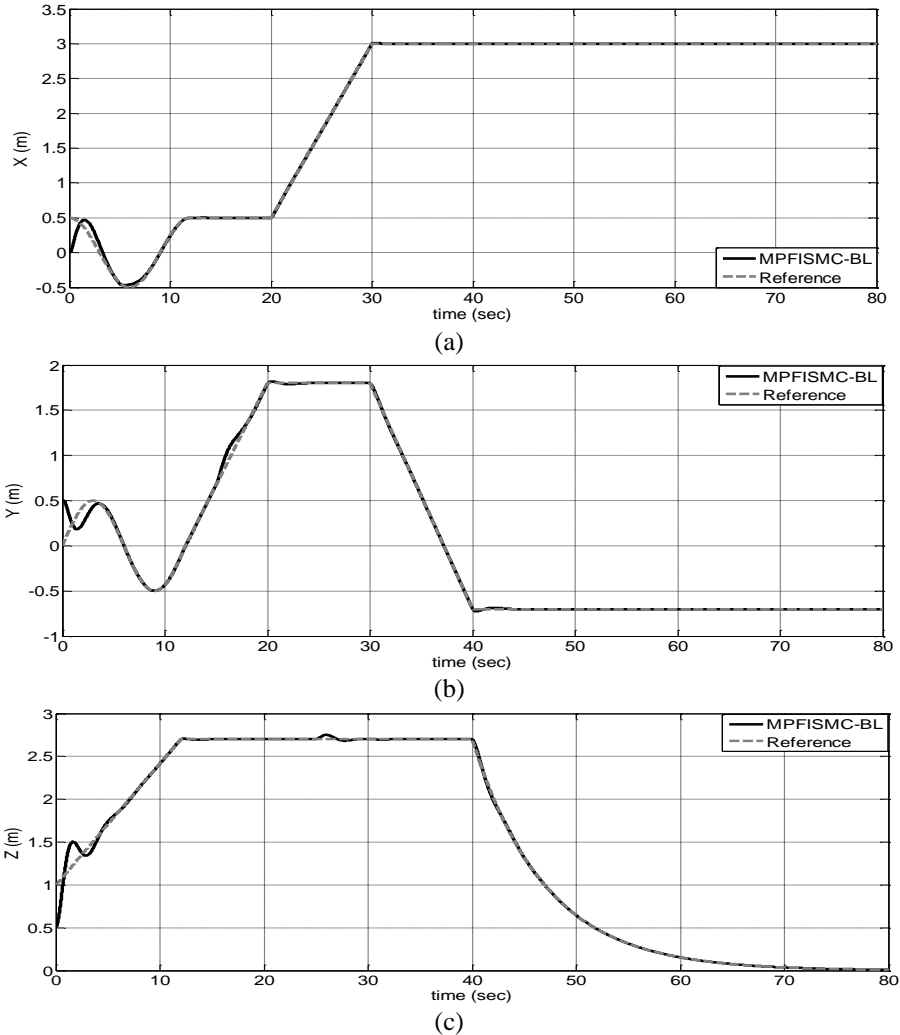


Fig. 6. Position (x, y, z) for quadrotor helicopter using MPFISM-C-BL.

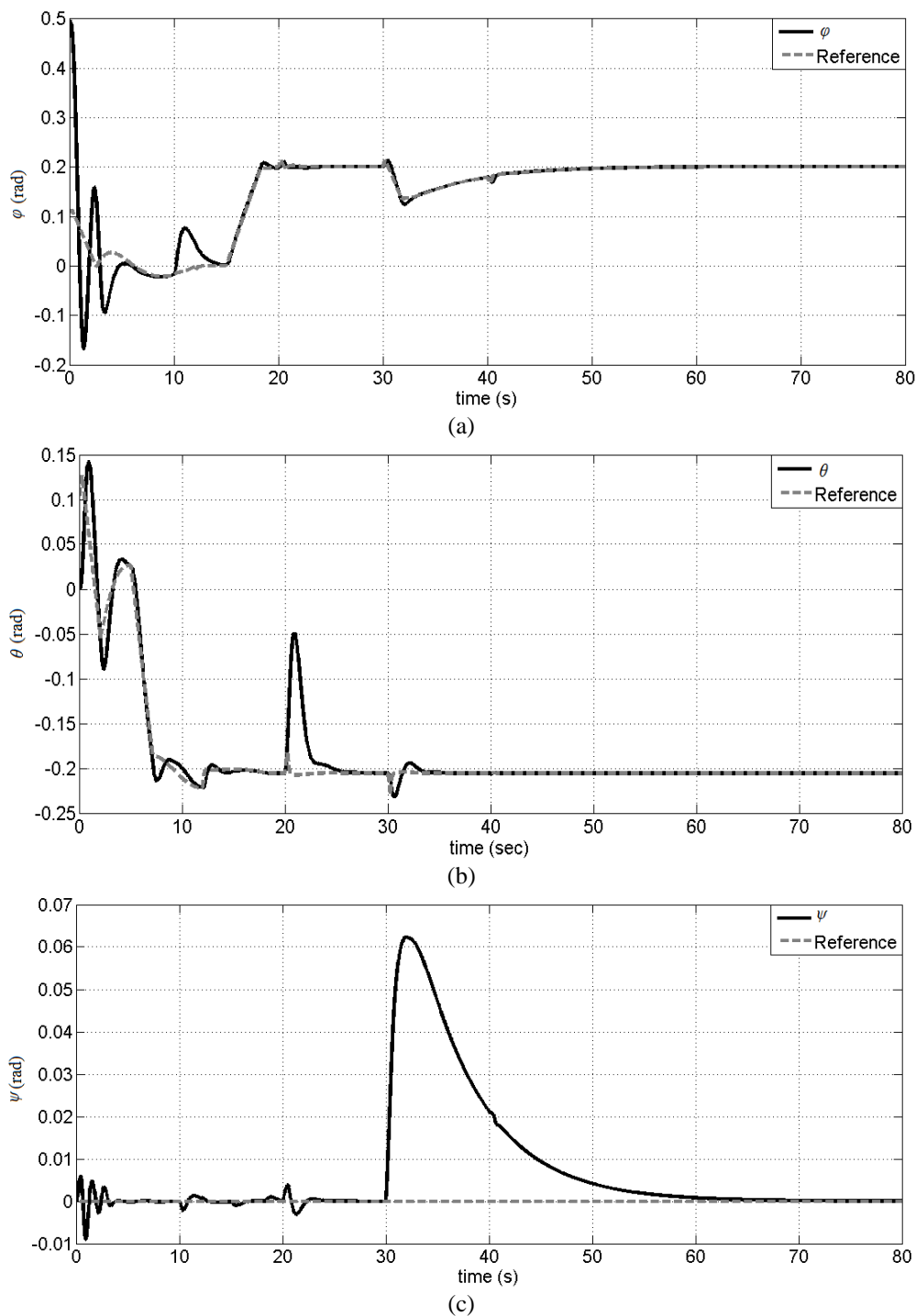
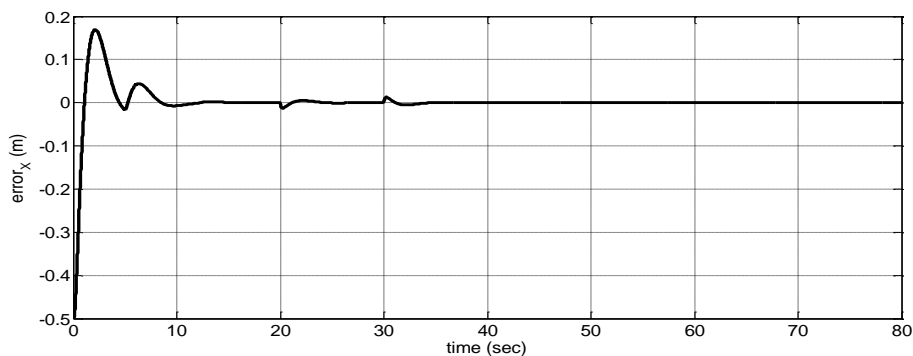


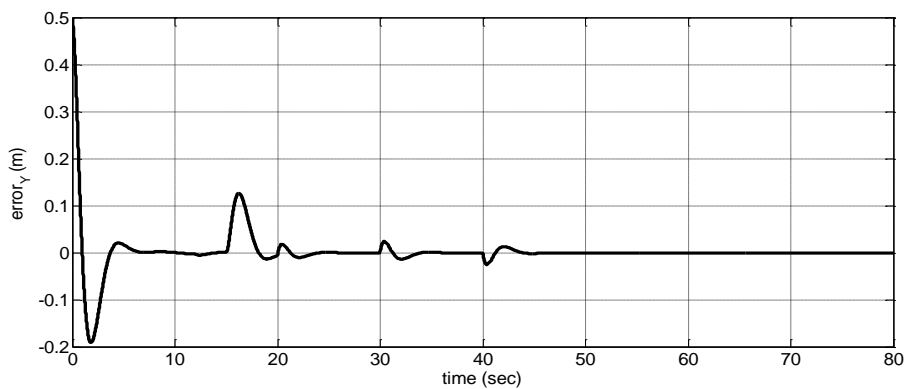
Fig. 7. Orientation ( $\varphi, \theta, \psi$ ) angles of quadrotor helicopter using MPFISM-C-BL.

The position and orientation errors of the quadrotor helicopter using MPFISM-C-BL are shown in Figs. 8 and 9, respectively. In order to evaluate the achieved

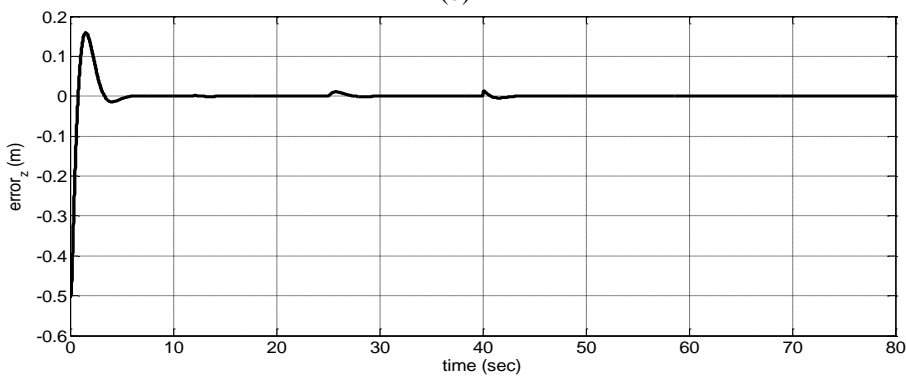
results, integral square error (ISE) is attained in the following.



(a)

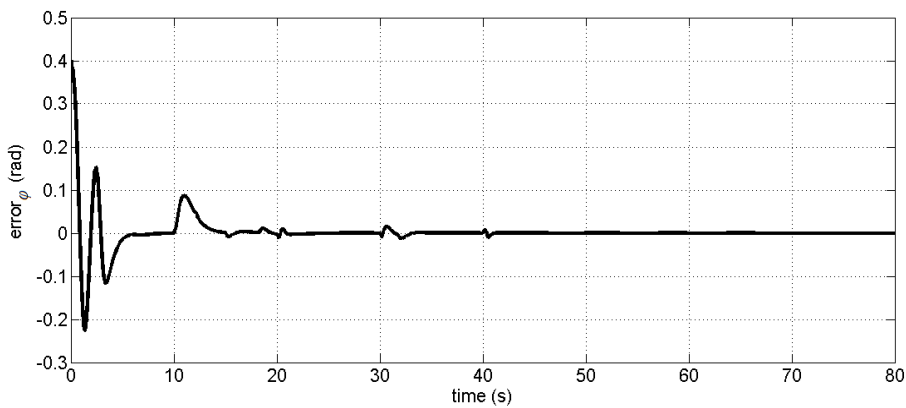


(b)



(c)

Fig. 8. Position errors for quadrotor helicopter using MPFISM-C-BL.



(a)



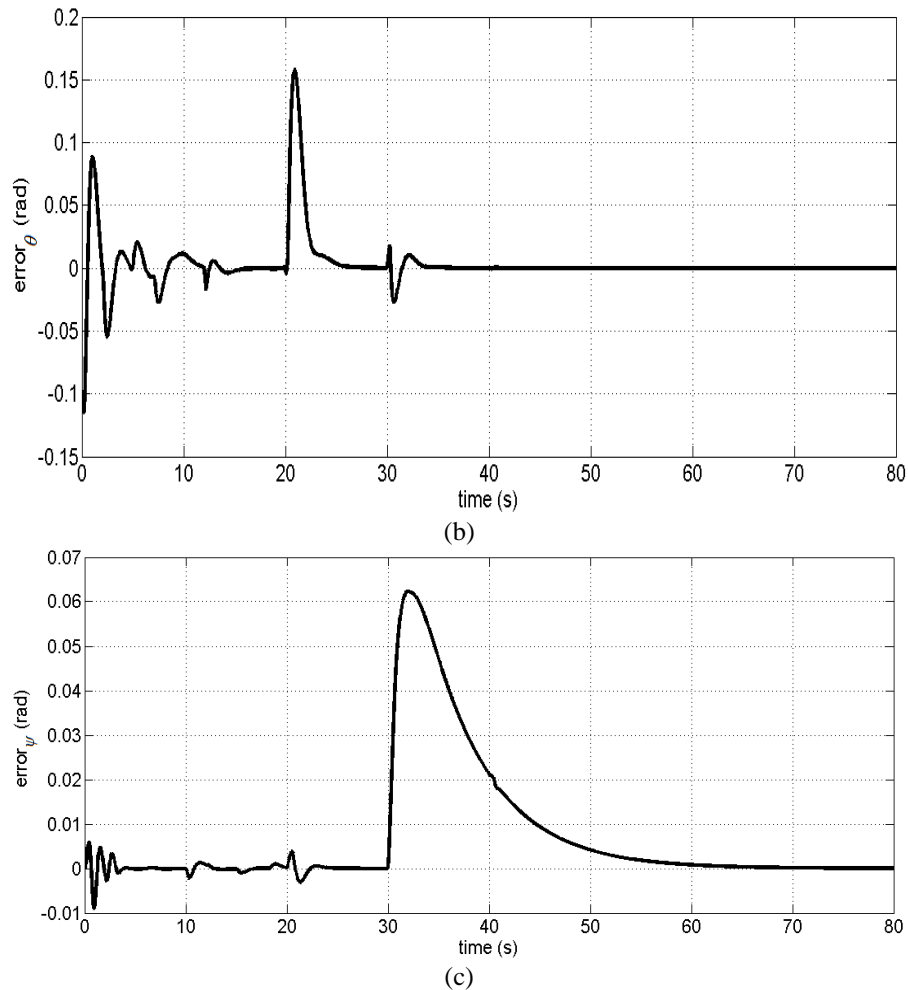


Fig. 9. Orientation errors for quadrotor helicopter using MPFISM-BL.

Table 3 shows the integral square error (ISE) performance indices attained from the simulation results.

Table 3. ISE performance analysis for quadrotor helicopter.

States	MPFISM-BL	MPC + NLH <sub>∞</sub> [75]	Back Stepping [75]
$x (m)$	14.8820	18.2883	26.1467
$y(m)$	13.7215	16.4420	22.0603
$z (m)$	10.6038	11.2947	19.0209
$\varphi (rad)$	13.1810	4.6388	19.4346
$\theta (rad)$	3.7235	4.7846	8.0633
$\psi (rad)$	2.1226	4.6225	5.2219

This table shows that the tracking error is improved by the MPFISM-BL controller. However, roll tracking is increased, due to nonlinearity and coupling in their desired input.

It is important to note that these results are attained by a linear model of the system for MPC with less calculation for MPFISM-BL.

Figure 10 shows control efforts for quadrotor helicopter using MPFISM-BL. Table 4 shows the integral absolute derivative control signal (IADU) index, computed for all control signals in control strategies. This index offers an appropriate check for smoothness of control signals. Based on Fig. 10 and Table 4, input control signals generated by MPFISM-BL control strategy are smoother than those of other controller strategies. However, roll control signals has more effort due to nonlinearity and coupling in their desired input.

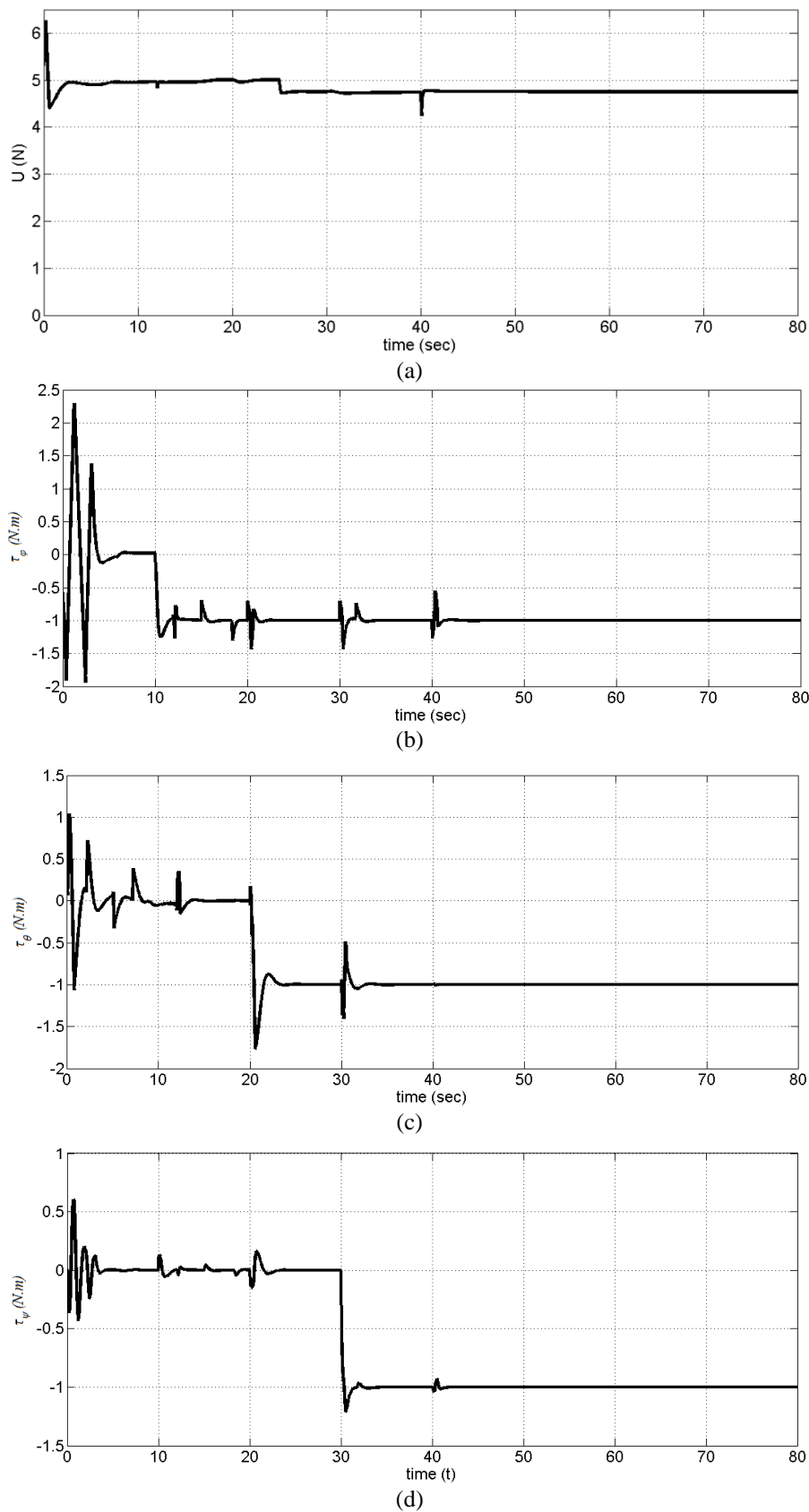
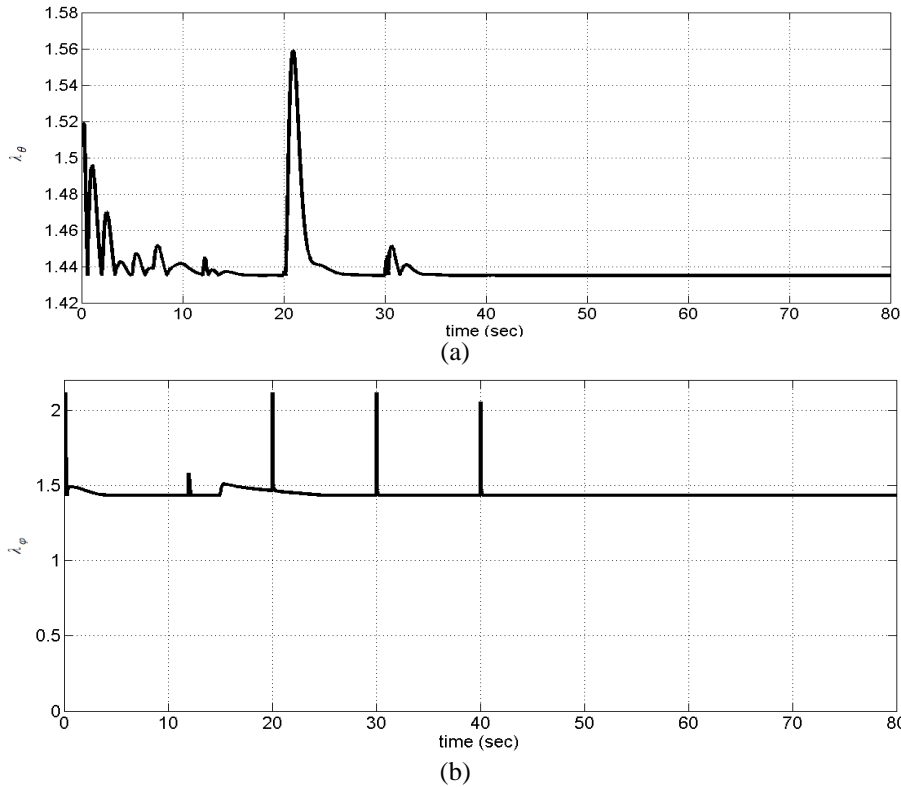


**Fig. 10.** Control inputs ( $U, \tau_\phi, \tau_\theta, \tau_\psi$ ) for quadrotor helicopter using MPFISM-C-BL.

**Table 4.** IADU performance analysis for quadrotor helicopter.

Control signals	MPFISM- BL	MPC + NLH <sub>∞</sub> [75]	Back Stepping [75]
$U$ (V)	17.2867	17.6692	20.8502
$\tau_{\phi_a}$ (N.m)	61.8308	63.9550	199.9717
$\tau_{\theta_a}$ (N.m)	64.8345	65.4172	220.3820
$\tau_{\psi_a}$ (N.m)	8.7451	18.7141	43.1515

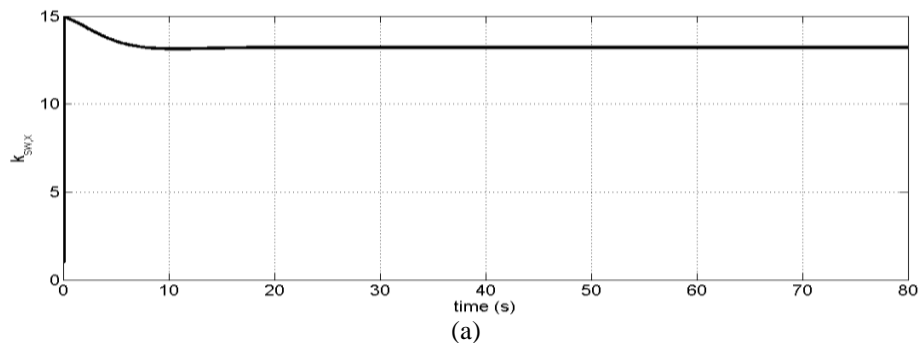
$\lambda_\theta$  and  $\lambda_\phi$ , which are designed by FLC, are shown in Fig. 11, based on the input and output membership functions presented in Fig. 4. The fuzzy rules are as described in Table 2.

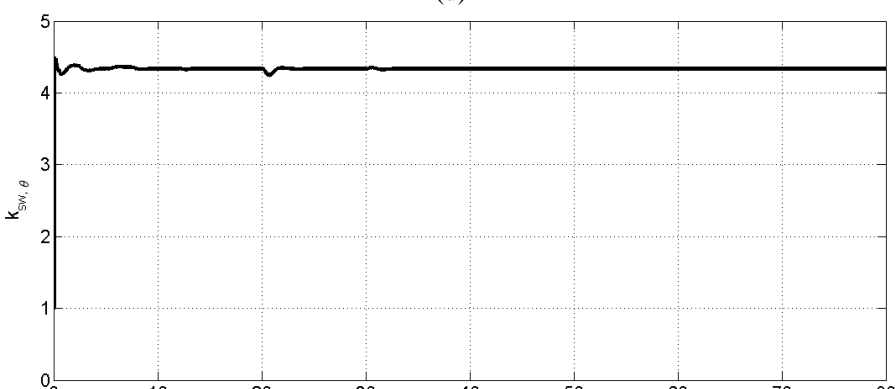
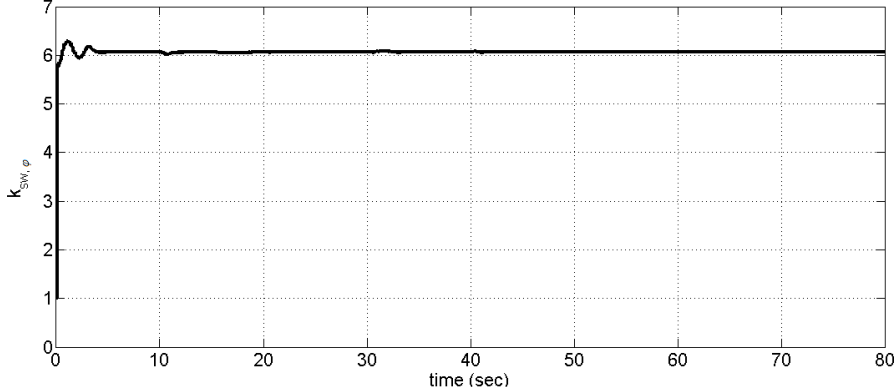
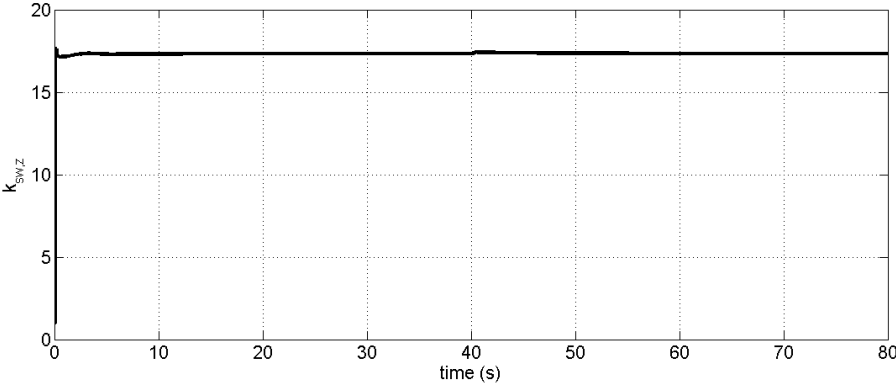
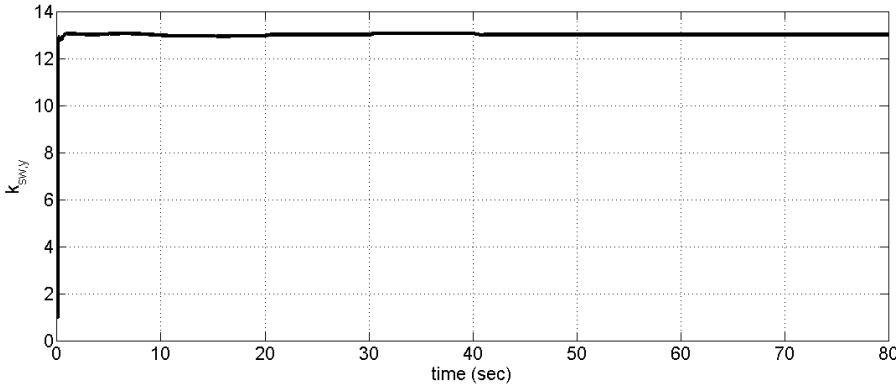


**Fig. 11.**  $\lambda_\theta$  and  $\lambda_\phi$  of MPFISM-*BL* designed by FLC.

The switching gains of MPFISM-*BL*, which are designed by MPC, are depicted in Fig. 12. This figure shows how on-line switching gains are updated to reach

optimal value based on cost functions and switching gain constraints.





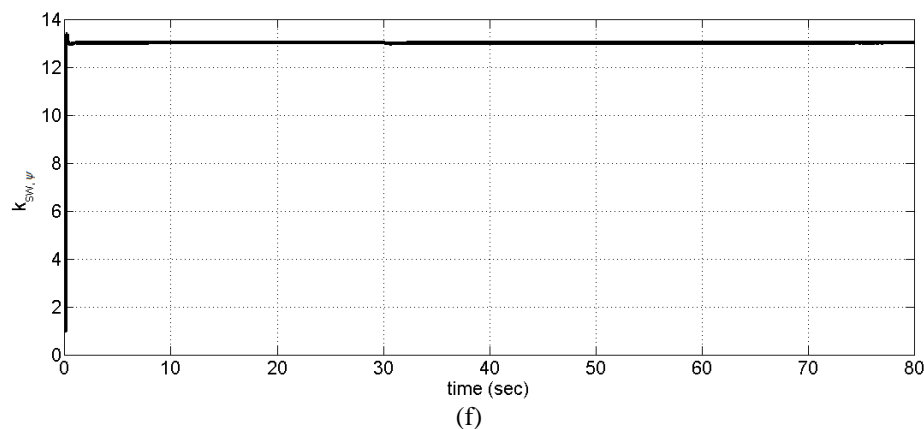


Fig. 12. The switching gains of MPFISM-C-BL designed by MPC.

## 5. CONCLUSION

The results reveal that the new merge of SMC with boundary layer (ISMC-BL), MPC, and FLC is an improved method for input tracking, optimization, and disturbance rejection performance for various applications such as the 6-DOF quadrotor helicopter.

The main outcome of this research is the introduction of a new robust, stable, optimal, and intelligent control scheme which is a multi-input model predictive fuzzy integral sliding mode control with boundary layer (MPFISM-C-BL). In this approach, a linear MPC, which considers constraints and cost function for optimal control performance at each sampling time, is used to design switching gains of control law. Moreover, equivalent control of MPFISM-C-BL deals with nonlinearity of the system. Besides, FLC is used to calculate the slope of sliding surface as an intelligent tool based on fuzzy rules.

## REFERENCES

- [1] J., Zhenyue, J., Yu, Yuesong Mei, Y., Chen, Y., Shen, and X., Ai. "Integral Backstepping Sliding Mode Control for Quadrotor Helicopter Under External Uncertain Disturbances," *Aerospace Science and Technology*, Vol. 68, pp. 299-307, 2017.
- [2] S., Bambang, N., Uchiyama, and Sh., Sano. "Least Square Based Sliding Mode Control for A Quadrotor Helicopter and Energy Saving by Chattering Reduction." *Mechanical Systems and Signal Processing*, Vol. 66, pp. 769-784, 2016.
- [3] A., Zaeri, A., Esmailian-Marnani, and S., Bahari Mohd Noor. "Improving Experimental Performance of Sliding Mode Control for a Two-Degree-of-Freedom Helicopter," *Majlesi Journal of Mechatronic Systems*, Vol. 6, no. 2, pp. 1-18, 2017.
- [4] M., Alireza, and M., Khodabandeh. "Adaptive Second Order Terminal Backstepping Sliding Mode for Attitude Control of Quadrotor with External Disturbances," *Majlesi Journal of Electrical Engineering*, Vol. 9, No. 2, pp. 51-58, 2015.
- [5] Toloei, A. R., M. Pirzadeh, and A. R. Vali. "Design of Predictive Control and Evaluate the Effects of Flight Dynamics on Performance of One Axis Gimbal System, Considering Disturbance Torques." *Aerospace Science and Technology*, Vol. 54, pp. 143-150, 2016.
- [6] S., Herwin, and B., Kusumoputro. "Direct Inverse Control based on Neural Network for Unmanned Small Helicopter Attitude and Altitude Control," *Journal of Telecommunication, Electronic and Computer Engineering (JTEC)*. Vol. 9, No. 2-2, pp. 99-102, 2017.
- [7] R., Nia Maharani, O., Wahyunggoro, and A., Imam Cahyadi. "Altitude Control for Quadrotor with Mamdani Fuzzy Model." In *Science in Information Technology (ICSITech), 2015 International Conference on*, pp. 309-314. IEEE, 2015.
- [8] S., Danial, S. M., Kargar, and S. M. A. Zanjani. "Mathematical Modeling and Designing PID Controller for a Quadrotor and Optimize its Step Response by Genetic Algorithm." *Majlesi Journal of Electrical Engineering*, Vol. 10, No. 4, 2016.
- [9] R., Guilherme V., Manuel G. Ortega, and Francisco R. Rubio. "An Integral Predictive/ Nonlinear  $H_{\infty}$  Control Structure for a Quadrotor Helicopter," *Automatica* Vol. 46, No. 1, pp. 29-39, 2012.
- [10] H. Bouadi, M. Bouchoucha, and M. Tadjine, "Sliding Mode Control based on Backstepping Approach for an UAV Type-Quadrotor," *International Journal of Applied Mathematics and Computer Sciences*, Vol. 4, no. 1, pp. 12-17, 2007.